Control of magnetic anisotropy in $Fe_{1-x}Co_x$ films on vicinal GaAs and $Sc_{1-y}Er_yAs$ surfaces

A. F. Isakovic, J. Berezovsky, and P. A. Crowell[a)]
School of Physics and Astronomy, University of Minnesota, 116 Church Street SE, Minneapolis, Minnesota 55455

L. C. Chen, D. M. Carr, B. D. Schultz, and C. J. Palmstrøm
Department of Chemical Engineering and Materials Science, 421 Washington Avenue SE, Minneapolis, Minnesota 55455

We demonstrate that two distinct surface contributions to the magnetocrystalline anisotropy can be used to control the magnetic properties of thin films of bcc $Fe_{1-x}Co_x$ grown on GaAs (100) and $Sc_{1-y}Er_yAs$ (100). The bare GaAs (100) surface has twofold symmetry, and $Fe_{1-x}Co_x$ films grown directly on it show a strong uniaxial magnetic anisotropy. Fourfold symmetry is restored in films grown on interlayers of $Sc_{1-y}Er_yAs$, in which the rock-salt structure provides a fourfold symmetric surface. A uniaxial magnetic anisotropy can be induced in this case by miscutting the substrate towards a {111} plane, so that vicinal steps run along a ⟨011⟩ direction. A simple Néel pair-bonding model describes the evolution of the anisotropy with the degree of miscut. For miscut GaAs (100) surfaces without interlayers, *both* the intrinsic anisotropy originating from the surface bonding and a step-induced term contribute to the total magnetic anisotropy. Depending on the orientation of the miscut, the step contribution can either enhance or partially suppress the intrinsic uniaxial anisotropy. © *2001 American Institute of Physics.* [DOI: 10.1063/1.1355320]

Ferromagnet–semiconductor heterostructures are valuable systems for the study of fundamental magnetism as well as critical elements in potential devices relying on spin injection into semiconductors. The boundary between a ferromagnet and a semiconductor is not necessarily abrupt, and the electronic structure of the interface results in dramatic effects on the magnetic properties of the ferromagnet.[1–3] In contrast, the evolution of ferromagnetism in thin films grown on metallic surfaces is more closely linked to surface morphology.[4–6] For example, the magnetocrystalline anisotropies observed for films on vicinal metallic surfaces are in reasonable agreement with the Néel pair-bonding model,[7] which accounts for the symmetry breaking due to missing bonds at the interface. In this article, we demonstrate how both morphology and surface bonding influence the magnetic anisotropy of ferromagnetic $Fe_{1-x}Co_x$ films grown on vicinal GaAs and $Sc_{1-y}Er_yAs$ surfaces.

Details of the growth procedure for $Fe_{1-x}Co_x$ on (2×4) reconstructed GaAs (100) or $Sc_{1-y}Er_yAs$ ($y=0.7$) have been reported previously.[8] The alloy compositions (~50%) and film thicknesses (~200 Å) were measured by Rutherford backscattering. Magnetic measurements were performed using either vibrating sample magnetometry (VSM) or the magneto-optic Kerr effect (MOKE). For films grown on flat GaAs (100) substrates, there is a marked uniaxial magnetocrystalline anisotropy that leads to a characteristic *split-loop* behavior for in-plane magnetic fields oriented close to the $[01\bar{1}]$ direction, which is the magnetic hard axis.[9] Typical easy and hard axis loops are shown in Fig. 1(A). As verified by transverse and longitudinal MOKE,[8] the jump observed at the split field H_s corresponds to a nearly 90° rotation of the magnetization from $[01\bar{1}]$ to close to [011] (the easy axis) as the magnetic field along $[01\bar{1}]$ decreases from the saturation limit. A simple coherent rotation model using the magnetic free energy density

$$F=K_\nu u_\eta^2 u_\delta^2+K_u u_\eta u_\delta-\mathbf{M}\cdot\mathbf{H}, \tag{1}$$

where K_ν and K_u are cubic and uniaxial anisotropies and u_η and u_δ are the direction cosines relative to [010] and [001], provides a good qualitative description of the hysteresis loops for all in-plane field orientations as well as a quantitative description of the dependence of the split field on field direction. (The demagnetizing energy $2\pi M^2$ is larger than any of the anisotropy energies, forcing the magnetization to lie in plane for all of the films discussed in this article. The measured saturation magnetizations are close to the value of 1900 emu/cm^3 found for bulk $Fe_{0.5}Co_{0.5}$ alloys,[10] and we will use this value for the analyses in this article.) For a typical film with $x=0.51$, $K_\nu=-2.2\times10^5$ erg/cm^3, and $K_u=-2.4\times10^5$ erg/cm^3. The large uniaxial anisotropy originates from the twofold symmetry of the GaAs surface, on which the As bonds run along the $[01\bar{1}]$ direction. The corresponding uniaxial magnetic anisotropy has been observed by several groups,[1–3] although there is no detailed understanding of the bonding mechanism leading to the observed [011] easy axis.

For $Fe_{1-x}Co_x$ on (100) $Sc_{1-y}Er_yAs$, which has the rock-salt structure and cubic surface symmetry, the magnetic anisotropy inferred from both VSM and MOKE measurements is almost perfectly fourfold.[8] We have found that a uniaxial anisotropy can then be induced by growing films on vicinal substrates miscut towards either the $(111)A$ or $(111)B$ surfaces, leading to monolayer steps running along the $[01\bar{1}]$ and [011] directions, respectively. [The $(111)A$ surface is a {111} plane with Ga polarity while the $(111)B$ surface has

a)Author to whom correspondence should be addressed; electronic mail: crowell@physics.umn.edu

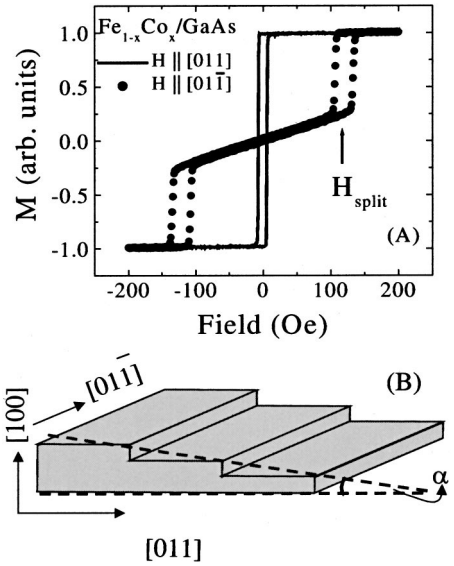

FIG. 1. (A) Typical hysteresis loops for $Fe_{1-x}Co_x$ ($x\sim0.50$) on GaAs(100) for applied fields H parallel to [011] (solid curve) and $[01\bar{1}]$ (points). The split field H_s is indicated by the arrow. (B) Schematic of a vicinal GaAs(100) substrate miscut toward (111)*A*. For (111)*B* miscuts, the steps are rotated 90°.

As polarity. The two miscuts differ by a 90° rotation.] A schematic of a vicinal (100) surface miscut toward (111)*A* is shown in Fig. 1(B). We have studied $Fe_{1-x}Co_x$ grown on $Sc_{1-y}Er_yAs$/GaAs with interlayer $Sc_{1-y}Er_yAs$ thicknesses of approximately 30 Å for vicinal angles $\alpha=0°-8°$. The miscut films show split loops similar to those observed for $Fe_{1-x}Co_x$ on flat GaAs (100), except that the magnitude of

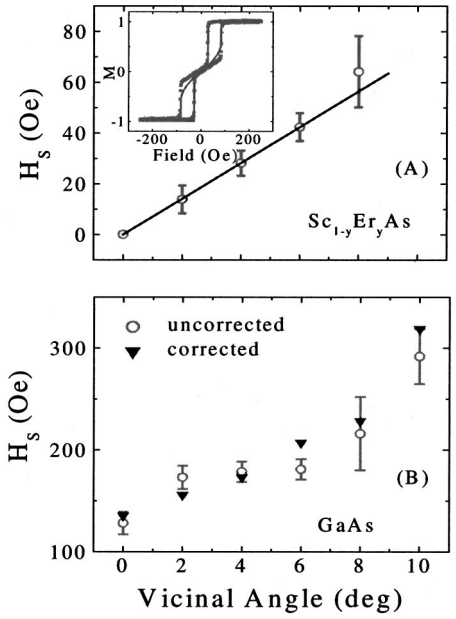

FIG. 2. (A) The split field (open circles) as a function of vicinal angle α for $Fe_{1-x}Co_x$ /$Sc_{1-y}Er_yAs$ on GaAs(100) miscut toward (111)*A*. The solid line is the split field as a function of angle from the model results. The inset shows the normalized magnetization (points) and model output for the anisotropy energy of Eq. (2) (solid curve) for a sample with $\alpha=8°$. (B) The split field (open circles) as a function of vicinal angle for $Fe_{1-x}Co_x$ /GaAs ($x\sim0.50$) miscut toward (111)*A*. The solid triangles are the same data normalized by multiplying by the sample thickness.

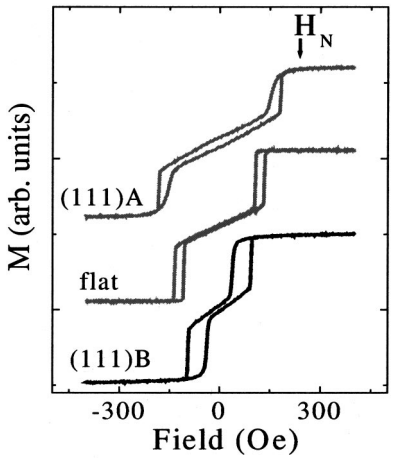

FIG. 3. Hysteresis loops for $H\|[01\bar{1}1]$ for $Fe_{1-x}Co_x$ ($x\sim0.50$) on vicinal GaAs (100). The middle curve shows the loop for a flat sample, and the top and bottom curves are for samples miscut 6° toward (111)*A* and (111)*B*. H_N indicates the field at which the parallel component of the magnetization begins to decrease in the (111)*A* sample.

the split field is much smaller, ranging from approximately 14 Oe at $\alpha=2°$ to 56 Oe at $\alpha=8°$. The split field H_s is shown as a function of the vicinal angle in Fig. 2(A). The easy axis is along [011], perpendicular to the steps.

We have modeled the magnetic reversal in these vicinal samples using an extension of the coherent rotation model adopted for the flat substrates. The uniaxial anisotropy is inferred from the Néel pair-bonding model,[7] assuming a free surface with monolayer steps (1/2 of a bcc unit cell) and an abrupt interface between $Fe_{1-x}Co_x$ and $Sc_{1-y}Er_yAs$. Since the steps on the $Sc_{1-y}Er_yAs$ surface are 1/2 of the rock-salt unit cell, which is almost exactly (within 1%) one $Fe_{1-x}Co_x$ unit cell, the steps on the semiconductor surface are twice as high as at the free surface. We follow Chuang *et al.*[7] in considering contributions to the anisotropy from missing bonds at surface sites and steps. Among these, only two types of step corner sites at a free (100) surface make a nonzero contribution to the anisotropy energy for steps running along $[01\bar{1}]$ or [011]. At the substrate surface, where the step is a full $Fe_{1-x}Co_x$ bcc unit cell high, there are four types of sites with missing bonds. These produce terms with the same symmetry as the free surface contributions, and so it is possible to reduce the number of pair-bonding parameters to two. We follow the standard practice of computing the an-

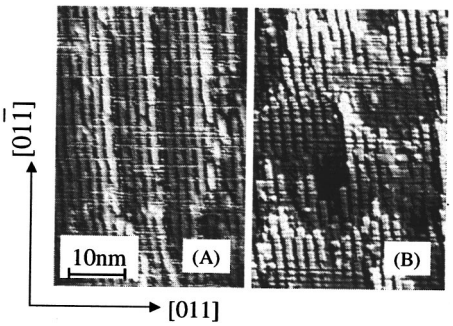

FIG. 4. Scanning tunneling microscope images of the surface steps on GaAs(100) miscut 2° toward (111)*A* (left) and (111)*B* (right).

isotropy energy in the lattice basis and then transforming to a set of experimental axes by an appropriate rotation.[6] For (100) surfaces miscut towards $(111)A$, the anisotropic part of the free energy density is $F_A = F_\nu + F_s$, where

$$F_\nu = K_\nu \left[\frac{1}{4}(u_x^4 + u_y^4) - \frac{1}{2}(1 - 3\alpha^2) u_x^2 u_y^2 + \frac{\alpha^2}{2} u_x^4 \right],$$

and (2)

$$F_s = \frac{1}{3d}[K_{s1}\alpha u_y^2 - (K_{s1}\alpha + 2\sqrt{2}K_{s2}\alpha^2) u_x^2].$$

The direction cosines u_x and u_y refer to the projections of $[011]$ and $[01\bar{1}]$ onto the semiconductor surface, and d is the $Fe_{1-x}Co_x$ thickness. We have retained terms to second order in the vicinal angle α. The effective surface anisotropies K_{s1} and K_{s2} originate from various combinations of the pair-bonding contributions from the different types of step sites. For each film, a series of in-plane rotation scans was conducted with the VSM and/or MOKE, and the hysteresis loops were fitted by mapping the evolution of the local minimum of the free energy $F = F_A - \mathbf{M}\cdot\mathbf{H}$ as the field was swept. The final parameters were averaged to arrive at a single set K_ν, K_{s1}, and K_{s2} for the entire group of vicinal samples. For samples miscut towards $(111)A$, the hard axis is $[01\bar{1}]$, and the final fitting parameters are $K_\nu = -6.6 \times 10^4$ erg/cm^3, $K_{s1} = 2.6$ erg/cm^2, $K_{s2} = 0.32$ erg/cm^2, with a saturation magnetization $M_s = 1900$ emu/cm^3. The average film thickness for this data set was $d = 180$ Å. A fit of a loop taken for H parallel to $[01\bar{1}]$ for $\alpha = 8°$ is shown in the inset of Fig. 2. We find that a single set of anisotropy parameters provides a good qualitative fit of the loops at all in-plane field orientations for vicinal angles above 4°. The modeling for smaller vicinal angles is handicapped by the fact that the experimental coercivities are generally much smaller than those predicted by the coherent rotation picture. As a final check, we can determine the split field analytically in the limits $\alpha \to 0$, $K_{s1}\alpha/3dK_\nu \ll 1$.[5] The result, $H_s = \alpha K_{s1}/3dM_s$, is shown as the solid curve in Fig. 2(A). The internal consistency of these results suggests strongly that the uniaxial anisotropy in these films is a surface component determined entirely by the degree of vicinality.

A similar set of split field data for $Fe_{1-x}Co_x$ on vicinal GaAs (100) *without* a $Sc_{1-y}Er_yAs$ interlayer is shown in Fig. 2(B). Since there was a relatively large thickness variation (13 Å out of an average thickness of 170 Å) in this set of samples, we show both the raw split field data as well as the split field multiplied by the film thickness. The fact that the normalization leads to a smoother data set suggests that the uniaxial anisotropy determining the split field is surface dominated, because any volume contribution should be independent of thickness. These data differ from those for films on $Sc_{1-y}Er_yAs$ in that there is a large uniaxial anisotropy $F_u = K_u u_x^2$ at zero miscut due to the twofold symmetric GaAs surface. This term changes only quadratically with the miscut angle and one would therefore expect the evolution with miscut to be dominated by the step contributions, linear in α, that were introduced in the previous paragraph. However, the fitting procedure described above fails to converge to a universal set of parameters for these films, suggesting that the steps actually modify the intrinsic uniaxial anisotropy.

We have also investigated the effects of miscuts towards the $(111)B$ surface. In this case, the steps run along $[011]$ instead of $[01\bar{1}]$. This changes the sign of the step-induced anisotropies K_{s1} and K_{s2} in Eq. (2). As expected, for films grown on $Sc_{1-y}Er_yAs$, this results in a rotation of 90° in the easy axis. For films grown directly on GaAs (100), the intrinsic uniaxial anisotropy is unchanged by the rotation, and the *total* uniaxial anisotropy should therefore decrease with increasing miscut. As shown in Fig. 3, the split field decreases when the substrate is miscut 6° toward $(111)B$, in agreement with this analysis. The distinction between the miscuts toward $(111)A$ and $(111)B$ is apparent in Fig. 4, which shows scanning tunneling microscope images of GaAs surfaces cut 2° off from (100). The (2×4) reconstruction, leading to As dimer rows running along $[01\bar{1}]$, is evident in both images. In the case of miscuts toward $(111)A$, the rows run parallel to the vicinal steps. For miscuts toward $(111)B$, the energy cost of cutting the dimer rows results in jagged step edges. Clearly, a correct microscopic treatment of this surface would go beyond the simple Néel model used here.

As is apparent in Fig. 3, the qualitative shape of the hysteresis loops for the miscut surfaces is fundamentally different from those obtained on flat substrates. In the flat substrate case, the nearly 90° rotation that occurs at the split field proceeds directly from the fully magnetized state as the magnetic field decreases. On the vicinal substrates, the jump is preceded by a continuous decrease in the magnetization, which is most likely due to the nucleation of easy axis domains near step edges, as was seen in the micromagnetic model of Hyman, Zangwill, and Stiles.[11] We observe a variety of other characteristic loops as a function of both the step density and in-plane field orientation. These will be discussed in greater detail in a future publication.

This work was supported in part by ONR Grant No. N/N00014-99-1-0233, DARPA/ONR Grant No. N/N00014-99-1005, the NSF MRSEC program under Grant No. DMR 98-09364, the Research Corporation, and the Alfred P. Sloan Foundation (PAC).

[1] E. M. Kneedler, B. T. Jonker, P. M. Thibado, R. J. Wagner, B. V. Shanabrook, and L. J. Whitman, Phys. Rev. B **56**, 8163 (1997).
[2] A. Filipe, A. Schuhl, and P. Galtier, Appl. Phys. Lett. **70**, 129 (1997).
[3] M. Dumm, M. Zolfl, R. Moosbuhler, M. Brockmann, T. Schmidt, and G. Bayreuther, J. Appl. Phys. **87**, 5457 (2000).
[4] A. Berger, U. Linke, and H. P. Oepen, Phys. Rev. Lett. **68**, 839 (1992).
[5] W. Weber, C. H. Back, A. Bischof, C. Wursch, and R. Allenspach, Phys. Rev. Lett. **76**, 1940 (1996).
[6] R. K. Kawakami, E. J. Escorcia-Aparicio, and Z. Q. Qiu, Phys. Rev. Lett. **77**, 2570 (1996).
[7] D. S. Chuang, C. A. Ballentine, and R. C. O'Handley, Phys. Rev. B **49**, 15084 (1994).
[8] L. C. Chen, J. W. Dong, B. D. Schultz, C. J. Palmstrøm, J. Berezovsky, A. Isakovic, P. A. Crowell, and N. Tabat, J. Vac. Sci. Technol. B **18**, 2057 (2000).
[9] C. J. Gutierrez, J. J. Krebs, and G. A. Prinz, Appl. Phys. Lett. **61**, 2476 (1992).
[10] *Magnetic Properties of Metals: d-Elements, Alloys, and Compounds*; edited by H. P. J. Wijn (Springer, Berlin, 1991).
[11] R. A. Hyman, A. Zangwill, and M. D. Stiles, Phys. Rev. B **58**, 9276 (1998).